**Annales
Geophysicae**

Different long-term trends of the oxygen red 630.0 nm line nightglow intensity as the result of lowering the ionosphere F2 layer

N. B. Gudadze, G. G. Didebulidze, L. N. Lomidze, G. Sh. Javakhishvili, M. A. Marsagishvili, and M. Todua

Georgian National Astrophysical Observatory, Ilia Chavchavadze State University, A. Kazbegi ave. 2a, 0160 Tbilisi, Georgia

Abstract. Long-term observations of total nightglow intensity of the atomic oxygen red 630.0 nm line at Abastumani (41.75° N, 42.82° E) in 1957–1993 and measurements of the ionosphere F2 layer parameters from the Tbilisi ionosphere station (41.65° N, 44.75° E) in 1963–1986 have been analyzed. It is shown that a decrease in the long-term trend of the mean annual red 630.0 nm line intensity from the pre-midnight value (+0.770±1.045 R/year) to its minimum negative value (−1.080±0.670 R/year) at the midnight/after midnight is a possible result of the observed lowering of the peak height of the ionosphere F2 layer electron density hmF2 (−0.455±0.343 km/year). A theoretical simulation is carried out using a simple Chapman-type layer (damping in time) for the height distribution of the F2 layer electron density. The estimated values of the lowering in the hmF2, the increase in the red line intensity at pre-midnight and its decrease at midnight/after midnight are close to their observational ones, when a negative trend in the total neutral density of the upper atmosphere and an increase in the mean northward wind (or its possible consequence – a decrease in the southward one) are assumed.

Keywords. Atmospheric composition and structure (Airglow and aurora) – Ionosphere (Ionosphere-atmosphere interactions; Mid-latitude ionosphere)

1 Introduction

Search for long-term trends of the atmosphere/ionosphere parameters is of vital importance for study of many solar-terrestrial coupling processes. Long-term variations in the upper atmosphere/ionosphere parameters may be related to environmental (anthropogenic/natural) changes in the troposphere (Roble and Dickinson, 1989; Rishbeth, 1990; Rish-

Correspondence to: G. G. Didebulidze
(didebulidze@genao.org)

beth and Roble, 1992; Bremer, 1998; Danilov and Mikhailov, 1999; Bremer and Berger, 2002; Bencze, 2005; Yue et al., 2006). The main cause of global warming in the troposphere is thought to be an increase in the density of the greenhouse gases (Roble and Dickinson, 1989; Rishbeth, 1990; Rishbeth and Roble, 1992). Besides anthropogenic agents, variations in the content of mineral dust aerosols and/or in the intensity of galactic cosmic rays which influence cloud covering in the troposphere have also been regarded as possible modulators of global warming (Marsh and Svensmark, 2000). Such environmental changes in the lower atmosphere are expected to affect the upper atmosphere temperature, charged and neutral particles densities, dynamics and the upper atmosphere-ionosphere coupling processes.

Recently, different long-term trends have been found in the oxygen red 630.0 nm line total nightglow intensity emitted from the ionospheric F2 region (Gudadze et al., 2007) after astronomical twilight and at midnight/after midnight by using photometrical observations made at Abastumani in 1957–1993. These phenomena are thought to be a possible consequence of lowering the ionosphere F2 layer, which was observed at several ionosphere stations (Ulich and Turunen, 1997; Bremer, 1998; Jarvis et al., 1998; Marin et al., 2001; Xu et al, 2004). The lowering in the ionosphere F2 layer, was predicted by Roble and Dickinson (1989), Rishbeth (1990), Rishbeth and Roble (1992) as the result of cooling in the upper atmosphere which should accompany global warming in the lower atmosphere. Later the presence of a positive long-term trend in hmF2 was also detected for some ionosphere stations (Bremer, 1998; Marin et al., 2001). According to an alternative approach to interpretation of the long-term ionospheric trends (called the geomagnetic control concept (Danilov and Mikhailov, 1999; Mikhailov, 2006, and references therein)), long-term variations in hmF2 are also controlled by geomagnetic activity variations. The negative trends in hmF2 revealed by Bremer (1998), Marin et al. (2001) for Western Europe (where

the magnetic declinations are negative) and the positive ones for Eastern European stations (where the magnetic declinations are positive) can be related to the enhanced westward thermospheric wind (Mikhailov, 2006). The recent results obtained by Emmert et al. (2004) show the presence of a secular negative trend in the upper atmosphere neutral gas density, which was independent of geomagnetic activity, local time, latitude and season. In spite of the observational evidence for the decrease in the upper atmosphere neutral gas density (Keating et al., 2000; Emmert et al., 2004; Marcos et al., 2005), which is considered to be the result of cooling of the upper atmosphere due to increase in the density of greenhouse gases in the lower atmosphere, there is still ongoing debate on whether anthropogenic or natural agents are crucial for determination of the trend of the ionosphere F2 region parameters (Lástovička et al., 2006; Mikhailov, 2006). The investigation of long-term variations in the red line intensity can give us additional information for resolving this problem because of their sensitivity to changes in physico-chemical processes in the upper atmosphere/ionosphere F regions.

In the present study, the existence of different trends of the annual mean value of the oxygen red line nightglow intensity observed at Abastumani (41.75° N, 42.82° E) is explained as the result of the negative trend of the ionosphere F2 layer peak height hmF2 observed over the neighbouring Tbilisi ionosphere station (41.65° N, 44.75° E). The theoretical interpretation of these phenomena as the result of the thermosphere mean northward meridional wind velocity increase (or consequently the decrease in the southward component) is proposed. In this case an increase in the northward component of meridional wind forces a downward plasma flux in the ionosphere F2 region, which causes the rapid increase in the ions (O_2^+) recombination rate at the lower heights of this region and corresponding increase in the red 630.0 nm line volume emission rate (responsible for the positive trend in its total nightglow intensity) at pre-midnight (after astronomical twilight). Such a quick damping of ions density gives its lower value in the red line emission layer at midnight and corresponding lower value of the total nightglow intensity of this line (responsible for its negative trend). The simulation will be done by use of a simple Chapman-type layer (damping in time) for the ionosphere F2 region electron density taking into account the meridional component of thermosphere wind. A secular decrease in the ionosphere F2 region neutral density (Emmert et al., 2004) accompanying the mid-latitude meridional wind field changes is considered as well.

2   The ionosphere F2 layer and the red 630.0 nm line intensity long-term trends

The mid-latitude atomic oxygen red 630.0 nm line is emitted from the ionospheric F2 region and the emission layer peak height is about 230–280 km (Fishkova, 1983). The red line nightglow intensity depends on the ionosphere F2

layer parameters. The long-term trend of the annual mean value of the atomic oxygen red 630.0 nm line total nightglow intensity was observed at Abastumani in 1957–1993 (Givishvili et al., 1996; Gudadze et al., 2007) and that of the ionosphere F2 layer peak height at the Tbilisi ionospheric station in 1963–1986 (Bremer, 1998). Unlike Givishvili et al. (1996), Gudadze et al. (2007) obtained another long-term trend at pre-midnight (after astronomical twilight) and midnight/after midnight. Going on this investigation allows us to compare the long-term trends of the ionosphere F2 layer parameters and the red line nightglow intensity obtained in these neighbouring places.

The main mechanism of excitation of mid-latitude oxygen atoms to the ^{1}D state O*(^{1}D $\xrightarrow{630\,\text{nm}}$ ^{3}P$_2$)during the nighttime is dissociative recombination of O_2^+ ions (Fishkova, 1983; Semeter et al., 1996; Didebulidze et al., 2002). This process along with collision deactivation of oxygen atoms O*(^{1}D) by the neutral particles (O, O_2, N_2) occurring in this region makes the 630 nm line intensity sensitive to different helio-geophysical conditions (Megrelishvili, 1981; Fishkova, 1983) including environmental changes in the lower atmosphere. Long-term variations in the red line intensity are related to many natural and anthropogenic processes. The variations in the solar ultraviolet radiation, geomagnetic activity and secular increase in the densities of the greenhouse gases in the lower atmosphere affect on the upper atmosphere temperature, neutral and charged particle densities, dynamics in the ionosphere F2 region, which in turn cause changes in the red 630.0 nm line nightglow intensity. In this case, there should be coupling between the long-term trends of the ionosphere F2 layer parameters and the red line nightglow intensity. In the following we will consider long-term variations in these parameters for the two neighbouring places, for which the ionosphere/thermosphere processes should be identical.

In Fig. 1 variations in the annual mean value of the red 630 nm line total nightglow intensity I_{630} (in Rayleighs) (upper panel), the ionosphere F2 layer peak height hmF2 (middle panel) and its electron density NmF2 (bottom panel) are plotted for three different pre-midnight periods (21:00–22:00 LT – full line and circles, 22:00–23:00 LT – thin line and diamonds and 23:00–24:00 LT – dashed line and "x"). Observations were made at Abastumani in 1957–1993 and Tbilisi in 1963–1986. For both Abastumani and Tbilisi, Local Time (LT)=Universal Time+3 h. The considered premidnight (after astronomical twilight) time interval includes the red line total nightglow intensity I_{630} observations for any month of the year. The maximum of the ionosphere F2 layer peak height hmF2 for Tbilisi ionosonde data (http://www.ukssdc.ac.uk/) was calculated by the Shimazaki (1955) empirical formula:

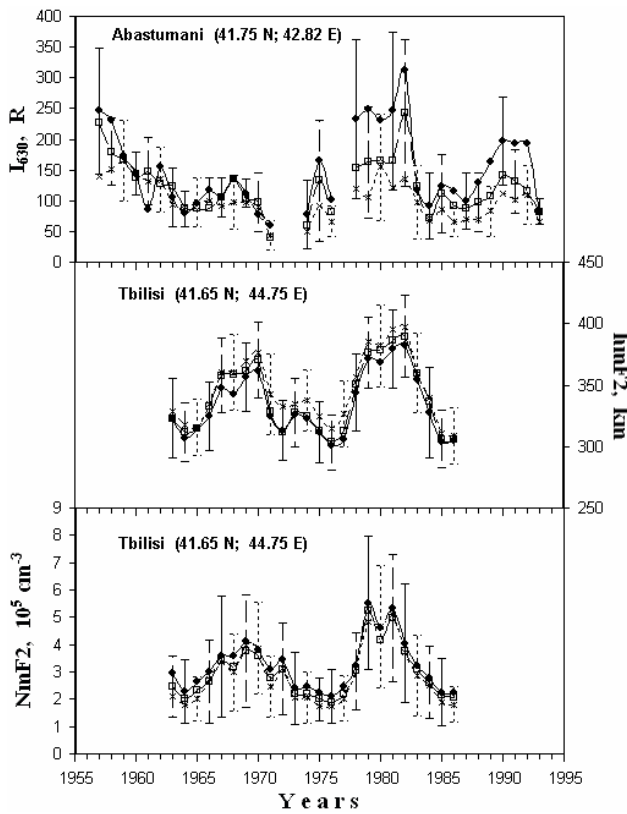$$hm\text{F2} = \frac{1490}{M(3000)\text{F2}} - 176, \tag{1}$$

Fig. 1. Variations of the annual mean value of the red 630 nm line total nightglow intensity I_{630} (upper panel), the ionosphere F2 layer peak height hmF2 (middle panel) and its electron density NmF2 (bottom panel) for three different pre-midnight periods (21:00–22:00 LT – full line and circles, 22:00–23:00 LT – thin line and diamonds and 23:00–24:00 LT – dashed line and "x") observed at Abastumani in 1957–1993 and Tbilisi in 1963–1986. Vertical lines are one sigma error bars.
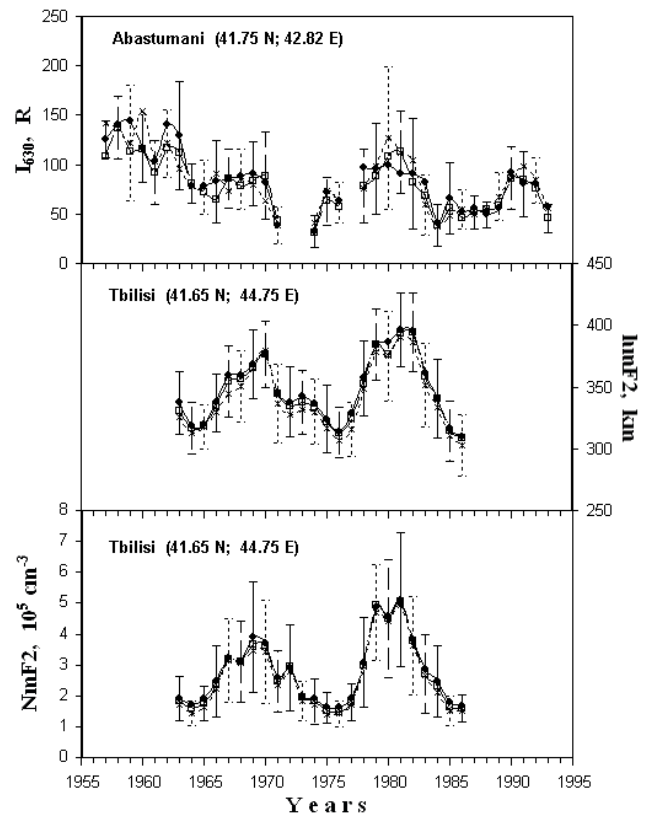
Fig. 2. Variation of the annual mean value of the red 630 nm line total nightglow intensity I_{630}, the ionosphere F2 layer peak height hmF2 and its electron density NmF2 for three after midnight periods (00:00–01:00 LT – full line and circles, 01:00–02:00 LT – thin line and diamonds and 02:00–03:00 LT – dashed line and "x") observed at Abastumani in 1957–1993 and Tbilisi in 1963–1986. Vertical lines are one sigma error bars.

where M(3000)F2 is the propagation factor (the ratio of the maximum usable frequency at a distance of 3000 km to foF2). In Fig. 1, instead of the ionosphere F2 layer critical frequency foF2, we have plotted for convenience the ionosphere F2 layer electron density peak value NmF2. As distinct from an early consideration by Givishvili et al. (1996), in Fig. 1 we have separated the pre-midnight time interval with comparatively quick variations in the mean annual red line intensity I_{630} which is also characterized by different long-term trends (Gudadze et al., 2007). We have also separated a time interval after midnight in which the red line intensity I_{630} and the ionosphere F2 layer parameters are close to equilibrium.

In Fig. 2 variations in the annual mean value of the red 630 nm line total nightglow intensity I_{630}, the ionosphere F2 layer peak height hmF2 and its electron density NmF2 are plotted for three after midnight periods (00:00–01:00 LT – full line and circles, 01:00–02:00 LT – thin line and diamonds and 02:00–03:00 LT – dashed line and "x"). Observations

were made at Abastumani in 1957–1993 and Tbilisi in 1963–1986.

Figures 1 and 2 show dynamical coupling between the ionosphere-thermosphere processes. The annual mean values of hmF2 increase and those of NmF2 and red line intensity I_{630} decrease with time from pre-midnight to midnight/after midnight period. This is more noticeable at pre-midnight when the electron density peak height hmF2 upwelling motion to its maximum value at midnight occurs. At midnight, when the ionosphere F2 region is more or less in equilibrium, the difference between the long-term variations in the hmF2 and the NmF2 is smaller in three separate time intervals after midnight than at pre-midnight. All these ionosphere F2 region parameters are sensitive to solar variability. From these figures we see an influence of the solar cycle on the long-term variations in the nightglow red line intensity I_{630} and the ionosphere F2 layer hmF2 and NmF2 parameters. The amplitude of solar cyclic variations in the mean annual red line intensity is greater at pre-midnight than at midnight/after midnight (Fig. 1). It remains about the same

at midnight/after midnight (Fig. 2). A similar difference is observed for the mean annual value of the ionosphere F2 layer peak electron density $NmF2$ and its height $hmF2$, but it is more noticeable in the red line intensity variations.

To separate the solar and geomagnetic effects from the trend of the annual mean value of the red line intensity, $hmF2$ and $NmF2$, by analogy with Gudadze et al. (2007), we use the following third-order regression equation

$$X_{th} = A + \sum_{i=1}^{3} B_i^{(1)} \cdot S_i + \sum_{j=1}^{3} \sum_{k=1(j\neq k)}^{3} B_{jk}^{(2)} \cdot S_j S_k + B^{(3)}$$
$$S_1 S_2 S_3 + C \cdot \text{Mag} + D \cdot \text{year} . \quad (2)$$

Here X_{th} corresponds to the mean annual theoretical value of $I_{630}/hmF2/NmF2$; S_1, S_2 and S_3 are the solar indices (www.spacewx.com) – the Wolf number R/the solar Lyman-α flux Ly_α/the solar radio flux $F_{10.7}$ (observed)/the solar EUV flux $E_{10.7}$ (observed) (Tobiska et al., 2000); $B^{(1)}(B_1^{(1)}, B_2^{(1)}, B_3^{(1)})$, $(B_{12}^{(2)} + B_{21}^{(2)}, B_{13}^{(2)} + B_{31}^{(2)}, B_{23}^{(2)} + B_{32}^{(2)})$ and $B^{(3)}$ are the coefficients describing variation of the solar indices of the first, second and third order, respectively; Mag describes the contribution of the planetary geomagnetic indices: A_p or the sum of the $K_p (\sum K_p)$ (www.ukssdc.ac.uk); A is the constant; D is the linear regression coefficient, which corresponds to the long-term trend of $I_{630}/hmF2/NmF2$. In the case of using the geomagnetic A_p index and its linear dependence on the only solar (Ly_α) index Eq. (2) is the same as used by Bremer and Berger (2002) for investigation of trend in the mesosphere LF phase-height long-term observations.

We also estimate the value of the long-term trend as in Bremer (1998). Assuming $D=0$ in Eq. (2), the long-term trend is estimated by the following expressions:

$$\Delta X = X_{\exp} - X_{th} \quad , \quad (3)$$

$$\Delta X = A_1 + D_1 \cdot \text{year} \quad , \quad (4)$$

where $X_{\exp}$ is the observational annual monthly mean value of $I_{630}/hmF2/NmF2$; D_1 is the linear regression coefficient, which corresponds to the trend of the considered ionosphere F2 regions parameters.

We can estimate trend values of $I_{630}/hmF2/NmF2$ by two methods. First, it is an estimation trend value D from Eq. (2), as done by Gudadze et al. (2007). In this case we choose such combination of the solar and geomagnetic indices so that the correlation coefficient (r) between $X_{\exp}$ and X_{th} is comparatively high ($r \geq 0.81$ for I_{630}, $r \geq 0.94$ for $hmF2$ and $NmF2$). Second, it is an estimation trend value D_1 from Eqs. (3) and (4), where X_{th} corresponds to the theoretical values obtained from Eq. (2), for $D=0$. In this case the geomagnetic and solar indices are chosen for a lower value in the standard deviation (or variance) of ΔX. Note that the lower value in the standard deviation (SD) of ΔX (SD$\leq$34 R for ΔI_{630}, SD$\leq$9.5 km for $\Delta hmF2$ and SD$\leq$0.236$\times 10^5$ cm^{-3} for $\Delta NmF2$) occurred

for the geomagnetic and solar indices which showed the above noted values of the correlation coefficient between the observational $X_{\exp}$ and theoretical X_{th} values of the upper atmosphere-ionosphere parameter $I_{630}/hmF2/NmF2$ estimated by the first method. Such estimations of these parameters are considered to be fittings to their observational values. So, Eq. (2) gives possibility to choose the first, second or third order description of the theoretical values of the $I_{630}/hmF2/NmF2$ through the solar indices and the planetary geomagnetic index.

The theoretical fitting is considered to be good for those solar and geomagnetic indices, which for most nighttime intervals (at least five from six considered hourly intervals in LT 21:00–03:00) gives the highest correlation between the theoretical and observational values ($0.81 \leq r \leq 0.87$ for I_{630} and 0.94–0.95$\leq r \leq$0.98–0.99 for $hmF2$ and $NmF2$) of the annual hourly means of the $I_{630}/hmF2/NmF2$ and the smallest values of corresponding SD (16 R$\leq$SD$\leq$34 R for ΔI_{630}, 6.4 km$\leq$SD$\leq$9.5 km for $\Delta hmF2$ and 0.126$\times 10^5$ cm^{-3} $\leq$ SD$\leq$0.236$\times 10^5$ cm^{-3} for $\Delta NmF2$) of ΔX (Eq. 3). Using two or three solar indices in Eq. (2) for estimation of annual hourly mean theoretical values of the $I_{630}/hmF2/NmF2$ increases the correlation between these parameters and their observational values in comparison with their description by one solar index. For some nighttime intervals the correlation coefficients between the theoretical and observational values of the red line nightglow intensity $I_{630}(t)$ increased from 0.74 to 0.86 while using one, two and three solar indices. Using two solar indices for the nighttime hourly mean value of $hmF2$ and $NmF2$ increases the correlation with its observed values from 0.94–0.95 up to 0.98–0.99. These correlation coefficients were also greater for most considered nighttime intervals (at least five from six considered hourly intervals in LT 21:00–03:00) for the mean annual values of the solar and geomagnetic indices calculated by their daily values for nights, when observations of the given upper atmosphere-ionosphere F2 layer parameters were available. A good fitting (with r and SD noted above) of the nighttime theoretical values of the $NmF2/hmF2$ to their observational ones occurs for (i) the solar EUV flux $E_{10.7}$, the Lyman-α flux Ly_α and the geomagnetic Ap indices (Ap, E, Ly), and (ii) the Lyman-α flux Ly_α, the Wolf number R and the geomagnetic Ap indices (Ap, R, Ly). The third-order description with the solar indices ($B^{(3)} \neq 0$), Eq. (2), of these ionosphere F2 layer parameters does not give any important changes in the value of the trend D in comparison with the second-order ($B^{(3)}=0$) description.

For the red line intensity, a good fitting of observational data ($0.81 \leq r \leq 0.87$, 16 R$\leq$SD$\leq$34 R) occurs for the third-order regression Eq. (2) with the Wolf number R, the solar radio flux $F_{10.7}$, the Lyman-α flux Ly_α, the solar EUV flux $E_{10.7}$, the geomagnetic Ap indices and the sum of the planetary K_p indices ($\sum K_p$) in the following combinations: ($\sum K_p$, E, Ly, R), ($\sum K_p$, F, Ly, R), (Ap, E, Ly, R) and (Ap, F, Ly, R). Here a good fitting ($r \approx 0.85$, SD$\approx$33.9 R)

Table 1. Trends, mean correlation coefficients r (between X_{exp} and X_{th}), standard deviations (for ΔX) of the mean annual oxygen red 630.0 nm line nightglow intensity I_{630} observed at Abastumani (41.75° N; 42.82° E) in 1957–1993 and the ionosphere F2 layer peak electron density NmF2 and its height hmF2 observed at Tbilisi (41.65° N, 44.75° E) in 1963–1986 at pre-midnight and after midnight for different solar and geomagnetic indices. The trend values are given with their errors at 95% confidence level.

Time interval LT	I_{630}				hmF2				NmF2			
	(Ap,E,Ly,R) trend, R/year	(Ap,F,Ly,R) trend, R/year	r	SD, R	(Ap,E,Ly) trend, km/year	(Ap,R,Ly) trend, km/year	r	SD, km	(Ap,E,Ly) trend, 10^5 cm^{-3}/year	(Ap,R,Ly) trend, 10^5 cm^{-3}/year	r	SD, 10^5 cm^{-3}
21:00–22:00	+0.780±1.047 (ΣKp,E,Ly,R)	+0.764±1.043 (ΣKp,F,Ly,R)	0.85	33.9	−0.492±0.429	−0.465±0.439	0.95	8.1	−0.0109±0.0132	−0.0097±0.0132	0.97	0.236
22:00–23:00	−0.271±0.925	−0.329±0.925	0.75	28.9	−0.505±0.474	−0.488±0.478	0.94	9.5	−0.0070±0.0131	−0.0067±0.0133	0.97	0.216
23:00–24:00	−0.826±0.645	−0.859±0.641	0.82	19.1	−0.444±0.348	−0.440±0.354	0.96	7.7	−0.0031±0.0125	−0.0041±0.0131	0.98	0.207
00:00–01:00	−1.073±0.671	−1.084±0.668	0.81	18.1	−0.459±0.325	−0.448±0.334	0.97	6.7	−0.0029±0.0092	−0.0039±0.0099	0.99	0.156
01:00–02:00	−0.948±0.539	−1.013±0.545	0.85	16.5	−0.437±0.332	−0.441±0.337	0.97	6.4	−0.0038±0.0091	−0.0047±0.0097	0.99	0.155
02:00–03:00	−0.814±0.584	−0.926±0.595	0.87	16.9	−0.465±0.430	−0.465±0.436	0.97	7.0	−0.0029±0.0070	−0.0038±0.0080	0.99	0.126

of experimental values of the mean annual red line nightglow intensity for the planetary geomagnetic Ap indices occurs at 21:00–22:00 LT. In general, the red line intensity is more sensitive to variation in the sum of the planetary Kp indices (ΣKp). Taking into account the presence of planetary geomagnetic indices (Ap or ΣKp) in the regression Eq. (2) we get greater correlation coefficient between observational and theoretical values for the mean annual hmF2 by up to 2% and for the red line nightglow intensity by up to 5% than in the case of the absence of these indices. In this case, for the nighttime interval considered the correlation between the theoretical and observed values for the third-order regression equation for I_{630} with the solar indices increases by up to 12% and 5% as compared with the linear and second-order regression equations, respectively. The nonlinear (third-order) dependence of the red line intensity on the solar indices, Eq. (2), may result from its dependence on the ionosphere F2 region neutrals and ions temperature, electron N_e and ambient neutrals densities, for which long-term variations is possible to be described by different solar indices.

The trend values D of the mean annual I_{630}/hmF2/NmF2 and their errors for the considered parameters estimated by Eq. (2) (Gudadze et al., 2007) for most nighttime intervals are little greater than those for trend D_1 obtained by Eqs. (3) and (4). The latter with mean correlation coefficients (between X_{exp} and X_{th}) and SD for ΔX are summarized in Table 1.

In Table 1 the trends and their errors are given at 95% confidence level. The red line intensity trend at midnight/after midnight is always negative with a minimum value of about −1.080±0.670 R/year and it increases up to a positive value of about +0.770±1.045 R/year (85% confidence level for positive values) at pre-midnight. The trend of the nighttime ionosphere F2 layer electron density peak height hmF2 is always negative (at 95% confidence level) and its mean value for the considered time interval (LT 21:00–03:00) is about −0.455±0.343 km/year.

In the same nighttime interval the trend in the maximum electron density NmF2 is also negative but insignificant ((−0.00540±0.00986)×10^5 cm^{-3}/year). The trend value in the critical frequency foF2 ($\sim Nm$F2$^{1/2}$) for the nighttime interval (LT 21:00–03:00) is also negative and insignificant, which is not for brevity considered here.

Using Eqs. (3) and (4) for the same solar and geomagnetic indices (Ap, Ly_α, $E_{10.7}$ or Ap, Ly_α, R) the daytime (LT 10:00–14:00) trends are: −0.375±0.421 km/year in hmF2 (negative at 90% confidence level) and (−0.0082±0.0260)×10^5 cm^{-3}/year in NmF2, negative but insignificant. The average day-night (LT 00:00–23:00) trends in mean annual hmF2 and NmF2 are −0.402±0.319 km/year (negative at 98% confidence level) and (−0.0071±0.0157)×10^5 cm^{-3}/year (negative but insignificant), respectively. Note, that the same formalism of trend estimation of these parameters using the Wolf number R and geomagnetic Ap indices give −0.210±0.386 km/year and (0.0134±0.0273)×10^5 cm^{-3}/year, which are insignificant. The average day-night trend of mean monthly hmF2 at the Tbilisi ionosphere station obtained by Bremer (1998) using the same solar and geomagnetic indices is negative and also noted as insignificant.

The presence of the negative long-term trend of the ionosphere F2 layer electron density peak height hmF2 was detected at many ionosphere stations in different regions of the world (Ulich and Turunen, 1997; Bremer, 1998; Jarvis et al., 1998; Marin et al., 2001; Xu et al., 2004). This lowering of the ionosphere F2 layer may be the result of global cooling of the upper atmosphere (Roble and Dickinson, 1989; Rishbeth, 1990) and related changes in its dynamics. The negative trend observed in hmF2 (Table 1) and corresponding F2 layer lowering by about 15–19 km for 1957–1993 are greater than predicted by Rishbeth (1990), Rishbeth and Roble (1992) considering only the effect of the cooling in the upper atmosphere due to an increase in the content of greenhouse gases (CO_2 and CH_4) in the lower atmosphere. The

presence of such a negative trend in the hmF2 and the difference of pre-midnight and after midnight trend in the oxygen red line intensity at these two neighbouring stations may be attributed to changes in the meridional wind velocity.

A theoretical estimation of influence of the mean northward wind increase or decrease in the southward on lowering the hmF2 and accompanying difference between the pre-midnight and midnight/after midnight long-term trends of the oxygen red 630.0 nm line intensity will be made in the next section.

3   Theoretical simulation

The revealed important difference between the pre-midnight and midnight/after midnight long-term trends of the annual mean value red 630.0 nm line total nightglow intensity I_{630} is accompanied by lowering the ionosphere F2 layer peak height hmF2. To interpret these processes, we employ the analytic expressions for the red 630.0 nm line nightglow volume emission rate (VER) (Semeter et al., 1996; Didebulidze et al., 2002)

$$\varepsilon_{630} = f(^1\mathrm{D}) \left(\frac{A_{630}}{A_{^1\mathrm{D}}} \right)$$
$$\frac{s_1[\mathrm{O}_2](h) \cdot N_e(h,t)}{1 + d_{N2}[\mathrm{N}_2](h) + d_{O2}[\mathrm{O}_2](h) + d_O[\mathrm{O}](h)}, \quad (5)$$

and its total nightglow intensity

$$I_{630}(t) = 10^{-6} \int \varepsilon_{630}(h,t)dh. \quad (6)$$

Here t and h are the time and the height, respectively.

$s_1 = 3.23 \times 10^{-12} \exp[3.72 \left(300/T_i\right) - 1.87 \left(300/T_i\right)^2]$, T_i is the ionosphere F2 region ion temperature; d_{N2}, d_{O2} and d_O are the coefficients of collision deactivation of $O^*(^1\mathrm{D})$ by N_2, O_2 and O, respectively; $d_{N2} = s_2/A_{^1\mathrm{D}}$, $d_{O2} = s_3/A_{^1\mathrm{D}}$ and $d_O = s_4/A_{^1\mathrm{D}}$. $s_2 = 2.0 \times 10^{-11} \exp\left(107.8/T_n\right) \mathrm{cm}^3/\mathrm{s}$, $s_3 = 2.9 \times 10^{-11} \exp\left(67.5/T_n\right) \mathrm{cm}^3/\mathrm{s}$. $A_{^1\mathrm{D}}$ is the total transition coefficient $(A_{^1\mathrm{D}} = A_{630} + A_{636.4} + A_{639.2} = 7.45 \times 10^{-3} \mathrm{s}^{-1}$, $A_{630} = 5.63 \times 10^{-3} \mathrm{s}^{-1}$, $A_{636.4} = 1.82 \times 10^{-3} \mathrm{s}^{-1}$, $A_{639.2} = 8.93 \times 10^{-7} \mathrm{s}^{-1}$). The value of quantum yield, $f(^1\mathrm{D})$, is the mean number of excited atoms, $O(^1\mathrm{D})$, produced per recombination of O_2^+. Below, for the value of quantum yield we use $f(^1\mathrm{D}) \approx 1.1$ (Sobral et al., 1993).

From Eqs. (5) and (6) the red line VER $\varepsilon_{630}(h,t)$ and total nightglow intensity $I_{630}(t)$ depend on the temperatures of ambient ions (T_i) and neutrals (T_n), the densities of neutrals N_2, O_2 and O, and the F2 layer electron density $N_e(h,t)$. The different trends observed in the red line total nightglow intensity at pre-midnight and midnight/after midnight show that the resulting influence of the variations in these upper atmosphere-ionosphere F2 region parameters on the red line intensity should be different for the various nighttime intervals.

The night variation of the red line intensity (noticeable from Figs. 1, 2 as well) is mainly determined by the behaviour of the ionosphere F2 region electron density $N_e(h,t)$ (Didebulidze at al., 2002). The average densities of the neutrals N_2, O_2 and O at these regions of the thermosphere increase by a factor of up to 7 from solar minimum to solar maximum (Hedin, 1991), but their daily variations are smaller than those of the electron density $N_e(h,t)$. The upwelling motion of the electron density peak height hmF2 up to midnight corresponds to the rapid decrease in the VER $\varepsilon_{630}(h,t)$ (Eq. 5) and in the total nightglow intensity $I_{630}(t)$ (Eq. 6). The mean peak height hmF2 is the highest at midnight (see Fig. 2). The corresponding mean value of the electron density (including the NmF2) is large at 21:00–22:00 LT and then it decreases up to midnight (Fig. 1). This electron density decrease is larger at the lower heights where the neutral density is higher and lessens with increasing height due to diminution in the neutral molecular density. In this case, the midnight red line intensity is also close to equilibrium, according to Eqs. (5) and (6).

According to above considered variations in the peak height hmF2 should be one of the important events affecting the nighttime behavior of the red line intensity and its long-term variations. The long-term trend in hmF2 should also be the main factor causing different trends in the red line intensity for pre-midnight and midnight/after midnight time. The negative trend observed in the hmF2 gives corresponding mean long-term lowering of the ionosphere F2 layer. This phenomenon in turn gives an increase of the rates of ion recombination and production of $O^*(^1\mathrm{D})$ atoms for some time interval after astronomical twilight (pre-midnight), when charged particle densities in the F2 region is comparatively high during night (seen from Fig. 1 as well). This can result in enhancement in the red line VER $\varepsilon_{630}(h,t)$ (Eq. 5) and total intensity $I_{630}(t)$ (Eq. 6) and then their quick fall due to increase in molecule densities for lower heights of this region of the upper atmosphere. In this case the comparatively lower heights for the F2 layer at midnight/after midnight time give smaller densities of charged particles and corresponding smaller values in the red line intensity resulting in its negative trend.

A secular decrease in the upper atmosphere temperature and neutral gas density predicted by Roble and Dickinson (1989), as a result of the growth in the densities of greenhouse gases, also causes a lowering of the F2 layer (Rishbeth, 1990; Rishbeth and Roble, 1992). According to above consideration this phenomenon (lowering in the hmF2) should cause the increase in the value of the red line intensity at pre-midnight and its decrease at midnight/after midnight. Recently the secular negative trend in the upper atmosphere neutral gas density was observed by Emmert et al. (2004). The trends observed in the neutral gas density increase with height from 200–700 km, average values ranging from 2% to 5% per decade. According to this result, which is global, for the red line emission layer the decrease in the neutral

density of the mid-latitude ionosphere F2 region should be about 7.4–10% for the 37-year data set. The secular decrease in the upper atmosphere gas density obtained by Emmert et al. (2004) is close to the theoretical prediction by Akmaev and Fomichev (1998), Akmaev (2003). On the basis of these theoretical results a cooling of the upper atmosphere during 37 years should be up to 20 K for heights of the red line luminous layer, which is about 2% of the thermosphere temperature for this region (Hedin, 1991). According to the estimation by Rishbeth and Roble (1992), the lowering of the hmF2 over the next 100 years (assuming doubling in CO_2 density) was predicted to be about 15 km. Thus considering a linear decrease in the hmF2 it gives the lowering by about 6 km for 37 years. It means that the lowering of hmF2 by about 15–19 km observed for the Tbilisi ionosphere station for this time interval can not be explained only by the cooling of the upper atmosphere. An additional factor causing the lowering in the hmF2 is to be considered, which can be long-term changes of dynamical processes such as increase in the northward wind or decrease in the southward wind velocity, which provokes a downward drift of plasma in this region. The phenomena showing on long-term changes in the upper atmosphere wind are known. Recently, the mid-latitude mean mesosphere-lower thermosphere (MLT) northward wind velocity increase for some Northern Hemisphere regions has been revealed (Portnyagin et al., 2006). Earlier, a negative long-term trend of the ionosphere F2 layer peak height for two Southern Hemisphere sites was noted by Jarvis et al. (1998) and explained by the decrease in F2 layer altitude as a result of thermospheric cooling and the consequent fall in the altitude of fixed pressure levels. They also explained the reduced amplitude in diurnal variation of the F2 layer altitude by a reduction in the strength of the thermospheric wind.

The long-term increase in thermospheric mean northward wind velocity (or decrease in the southward) can provoke the downward motion of the ionosphere F2 layer (negative trend in the hmF2) and cause of different long-term trends in the red line intensity emitted from this region (Table 1). We investigate this phenomenon by use of the analytic expression for the height distribution of the mid-latitude nighttime ionosphere F2 layer electron density $N_e(h, t)$ (Didebulidze and Pataraya, 1999):

$$N_e(h, t) = N \cdot \exp\left[-\lambda(t - t_o) - \frac{z}{H} - \frac{\alpha}{2} \cdot e^{-\frac{z}{H}}\right] \quad . \quad (7)$$

This Chapman type distribution damping in time corresponds to the nonstationary solution of the ionosphere F2 region ambipolar diffusion equation, taking into account the meridional component (meridional wind) u_0 of background horizontal wind velocity of a neutral gas. In this case the equation of time decay λ and α parameters have the following form:

$$\lambda = \frac{V}{4H} \left\{\left[\left(\frac{u_o \sin\theta \cos\theta}{V}\right)^2 + 1\right]^{\frac{1}{2}} - \frac{u_o \sin\theta \cos\theta}{V}\right\}, \quad (8)$$

$$\alpha = \frac{VH}{D_o} \left\{\left[\left(\frac{u_o \sin\theta \cos\theta}{V}\right)^2 + 1\right]^{\frac{1}{2}} + \frac{u_o \sin\theta \cos\theta}{V}\right\}, \quad (9)$$

where $V = 2(\beta_o D_o)^{0.5}$ is the F2 layer specific velocity, $h = h_o + z$ is the height, h_o and t_o are some initial height and time, respectively, θ is the angle between the magnetic field and zenith (for Abastumani $\sin\theta \cos\theta \approx -0.4$). D_o, β_o are the coefficients of ambipolar diffusion and recombination at the height $h = h_o(z=0)$. The value of time decay λ (Eq. 8) corresponds to the mixing gas approach in the ionosphere F2 region (Didebulidze and Pataraya, 1999). The height hmF2 of the ionosphere F2 layer maximum electron density $(Nm$F2$=N_e(hm$F2$, t))$ is

$$hm\text{F2} = h_o + H \ln \alpha. \quad (10)$$

Equation (9) and (10) indicate that for the mean nighttime northward wind $(u_0 > 0)$ the electron density peak is comparatively lower than for the absence of the meridional wind $(u_0 = 0)$ and higher for the southward wind $(u_0 < 0)$. In other words increase in the northward wind (or decrease in the southward one) gives decrease (or lowering) in the peak height hmF2. From these equations, the increase of the northward wind velocity gives a decrease in the value of α and corresponding decrease in the hmF2 and vise versa, when there is an increase in the southward wind (or a decrease in the northward one) the electron density peak moves up.

From Eq. (8) the increase in the value of the northward wind velocity gives the increase in the value of λ. An upwelling or downward motion of the hmF2 due to long-term changes in the value of the meridional wind velocity u_0 gives corresponding different value in time decay λ of $N_e(h, t)$ (Eq. 7) and could be a result of a different trend in the red line VER $\varepsilon_{630}(h, t)$ (Eq. 5) and the integral intensity $I_{630}(t)$ (Eq. 6). Assumption of a long-term increase in the northward wind gives a lowering in the hmF2 and increase in λ, which could be responsible for pre-midnight positive trend of the red line intensity $I_{630}(t)$ and its negative value at midnight/after midnight. From Eqs. (5–8) the nightly behavior of the red line total intensity for two different values of the meriodional wind velocity u_{01} and u_{02} gives $I_{630}^{(1)}(t) = I_1 \exp[-\lambda_1(t - t_0)]$ and $I_{630}^{(2)}(t) = I_2 \exp[-\lambda_2(t - t_0)]$, respectively. Here I_1 and I_2 are the red line intensities at the initial time $t = t_0$ in the case of nightly mean meridional wind velocities u_{01} and u_{02}, respectively. λ_1 and λ_2 are the time decays of electron densities for u_{01} and u_{02}, respectively. From Eqs. (8) and (9) when $u_{02} > u_{01}$ then $\lambda_2 > \lambda_1$ and hmF2$(u_{02}) < hm$F2(u_{01}) for the same values of the parameters of the thermosphere-ionosphere F2 region. In this case the lower height of the F2 layer corresponds to the greater value in the neutral particle densities and corresponding greater values in the red line VER $\varepsilon_{630}(h, t)$ and integral intensity $I_{630}(t)$, which means that at some initial time after twilight (or pre-midnight) the condition $I_2 > I_1$ should take place. Equations (5) and (6) show that $I_2 > I_1$ takes
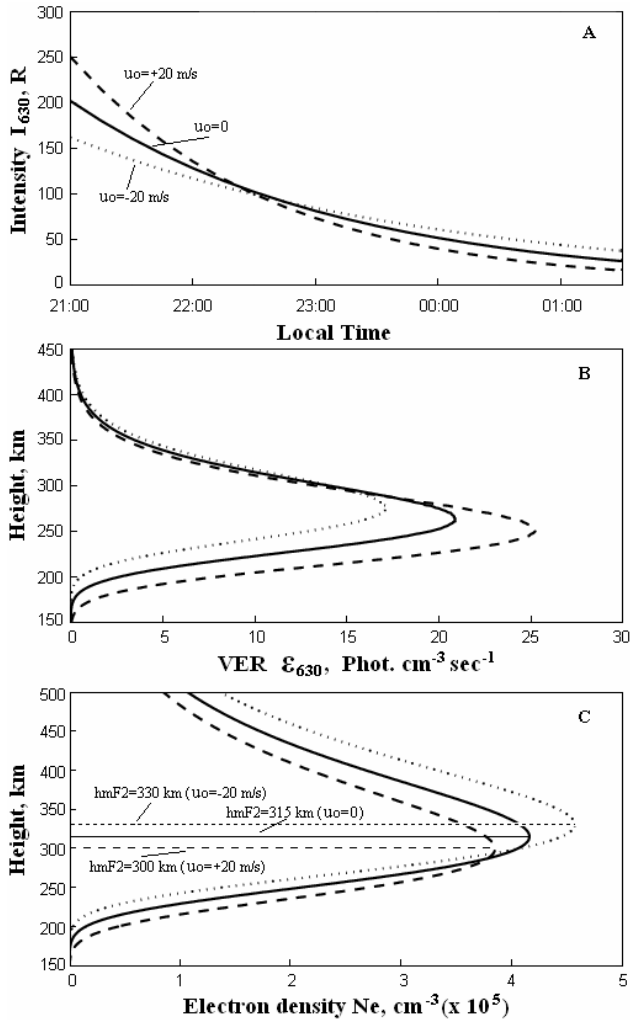
Fig. 3. Night variations of the red line total nightglow intensity $I_{630}(t)$ (panel **a**), height profile of the VER $\varepsilon_{630}(h)$ (panel **b**) and electron density $N_e(h, t=t_0)$ (panel **c**) for meridional velocity $u_0=-20$ m/s (dotted line), $u_0=0$ (full line) and $u_0=20$ m/s (dashed line).

place in the case of the lowering of the F2 layer either without changes in electron density $N_e(h, t)$ (Eq. 7) or when its decrease is comparatively smaller than the increase in the densities of neutrals (mainly [O_2]). If $I_2 > I_1$ and $\lambda_2 > \lambda_1$ then $I_{630}^{(1)}(t') = I_{630}^{(2)}(t')$ for some time of $t' > t_0$. For $t < t'$, $I_{630}^{(2)}(t) > I_{630}^{(1)}(t)$, which can result in a positive trend in the red line intensity, and for $t > t'$, $I_{630}^{(2)}(t) < I_{630}^{(1)}(t)$ we get a negative trend.

The lowering in the hmF2 and possibility of different values in the red line intensity trends can be shown using a similar formalism used above in the case of presence of a secular negative trend in the upper atmosphere neutral density and temperature. Below our theoretical estimations of the red line mean nightly behavior will include the cases of changes

in the meridional wind and these changes are accompanied by the cooling of the upper atmosphere.

In Fig. 3 the night variations of the red line total nightglow intensity $I_{630}(t)$ (panel a), height profile of the VER $\varepsilon_{630}(h)$ (panel b) and electron density $N_e(h, t=t_0)$ (panel c) for meridional velocity $u_0=-20$ m/s (dotted line), $u_0=0$ (full line) and $u_0=20$ m/s (dashed line), are plotted. Here $H=50$ km, $\beta_o=1.8 \times 10^{-4}$ s^{-1}, $D_o=9 \times 10^5$ m^2 s^{-1} and $h_o=294$ km. In this case $|u_0 \sin\theta \cos\theta| \approx 8$ m/s is of the same order as the specific velocity of the F2 layer $2(\beta_o D_o)^{0.5}=12.7$ m/s and the important changes take place in the electron density $N_e(h, t)$ (Eq. 7) time decay λ (Eq. 8) and peak height hmF2 (Eq. 9). In estimation we have chosen smaller values (by about 4%) in NmF2 for lower peak height at initial time LT 22:00. The peak height of the red line VER $\varepsilon_{630}(h, t=t_0)$ (Fig. 3b) is about 40–60 km lower than the height (hmF2) of the ionosphere F2 layer maximum electron density (NmF2) (Fig. 3c), which is typical for the mid-latitude height distribution of these parameters. The height profiles of the density of atomic oxygen [O](h), molecular oxygen [O_2](h) and molecular nitrogen [N_2](h) are chosen according to the MSISE-90 (Hedin, 1991) for some phase between solar maximum and minimum. Analytic approach (Eq. 7) is used for the height profile of the ionosphere F2 region electron density $N_e(h, t)$ (Fig. 3c).

The theoretical estimation in Fig. 3a reflects the typical nightly behavior of the red line intensity – its mean pre-midnight decrease from 150–300 R (the end of astronomical twilight) to about 30–70 R (midnight) at Abastumani (Fishkova, 1983). In this case an increase in the mean nightly northward wind or decrease in the southward one ($u_0=-20$ m/s; 0; 20 m/s) gives the increase in the pre-midnight total red line intensity I_{630} ($21h \leq t - t_o \leq 22h$) (Fig. 3a) and VER (Fig. 3b) and lowering in the peak height hmF2 (Fig. 3c). Such increase in the meridional wind gives an opposite picture for the red line intensity I_{630} ($t - t_o > 23h$) at midnight/after midnight – its value is smaller for greater northward wind velocities. Here the mean nightly meridional wind velocity can take values $u_0=-20$ m/s; 0; 20 m/s at different seasons and solar phases (Igi et al., 1999). This figure also shows that lowering in hmF2 by about 15 km, which is close to minimum value estimated from its trend (Table 1), gives an increase of the red line intensity by more than 30 R at LT 21:00–22:00. This value is greater than it will be predicted by observed trend value in the red line intensity (Table 1). Such simulation can easily be performed for any month. In the following similarly we will show a possibility of different trends observed in the red line intensity at pre-midnight and midnight due to changes in the meridional wind velocity and negative secular trend in the neutral density. We will demonstrate it for April, where the mean pre-midnight value of the red line intensity is between its minimum winter time and maximum summer time values (Fishkova, 1983).

In Fig. 4 the night variations of the red line intensity $I_{630}(t)$ observed in April (diamonds) and their theoretical values in the cases of: (i) $u_0=-25$ m/s, decrease in the densities of [N_2], [O_2] and [O] by 5% and temperature T_n by 1% (full lines); (ii) absence of decrease in the densities of neutrals and temperature (dotted lines), $u_0=-25$ m/s (panel a), $u_0=-14$ m/s (panels b and c), and (iii) decrease in the densities of neutrals by 10% and temperature by 2% (dashed lines), $u_o=-25$ m/s (panel b) and $u_0=-34$ m/s (panels b and c) are demonstrated. Estimating a decrease in the neutral densities [N_2], [O_2] and [O] by about the same value as obtained by Emmert et al. (2004) and decrease in the thermosphere temperature T_n we have taken into account the recombination and ambipolar diffusion coefficients according to the expressions (Nicolls et al., 2006):

$$\beta_o \propto s_1[O_2](h=h_0) + s_4[N_2](h=h_0), \tag{11}$$

$$D_o \propto T_n^{1/2}[O]^{-1}(h=h_0), \tag{12}$$

where $s_4=1.53\times10^{-12}-5.92\times10^{-13}\left(T_n/300\right)+8.6\times10^{-14}$ $\left(T_n/300\right)^2$ cm^3 s^{-1} (St.-Maurice and Torr, 1978), assuming $T_n\approx T_i$ for the heights of the red line luminous layer (Hedin, 1991). In this case the lowering in the hmF2 (Eq. 10) is about 7 km due to the decrease in the neutral densities by 10% and T_n by 2%, for the scale height H=50 km, β_o=1.8$\times10^{-4}$ s^{-1}, D_o=9$\times10^5$ m^2 s^{-1} and $u_0=-25$ m/s, (Fig. 4a). In this case using of mean height distribution of the F2 region neutral densities and temperature (in accordance with MSISE-90) for April at 1992–1993 (dashed lines), their values with 10% and 2% decrease (dotted lines), and 5% and 1% decrease for verification of mean observational results (full lines) allow us to demonstrate theoretically a possible development of the mean nightly behavior of the red line intensity during 1957–1993 at Abastumani. Such consideration gives lowering in hmF2 (up to 20 km), the $I_{630(t)}$ increase at pre-midnight LT 21:00–22:00 (by about 22 R) and its decrease at LT 23:00–01:00 (from -9 R to -20 R), close to their values estimated from trends (Table 1).

The mean nightly behavior of the red line intensity two/three hours before midnight or at midnight/after midnight is similar to those demonstrated in Figs. 3 and 4 for all seasons (Fishkova, 1983). The uncertainty δI_{630} in the theoretical value of I_{630} (Eq. 6) due to its seasonal or solar phase depending variations can be estimated by expression

$$\delta I_{630}(t) = I_{630}[N_e(\beta_o + \delta\beta, \ D_o + \delta D, \ u_o + \delta u; \ t);$$
$$[N_2] + \delta[N_2], \ [O_2] + \delta[O_2], \ [O] + \delta[O],$$
$$T_n + \delta T_n] - I_{630}[N_e(\beta_o, \ D_o, \ u_o; \ t); \ [N_2], \ [O_2], \ [O], \ T_n]$$

Here $\delta\beta$, δD and δu denote deviations of the recombination and ambipolar diffusion coefficients and meridional wind velocity for different season and solar phase from their values β_o, D_o and u_0 at the initial height $h=h_o$. The values of β_o, D_o, $\beta_o+\delta\beta$ and $D_o+\delta D$ are estimated by Eq. (11) and Eq. (12) for the mean neutral densities [N_2], [O_2], [O] and
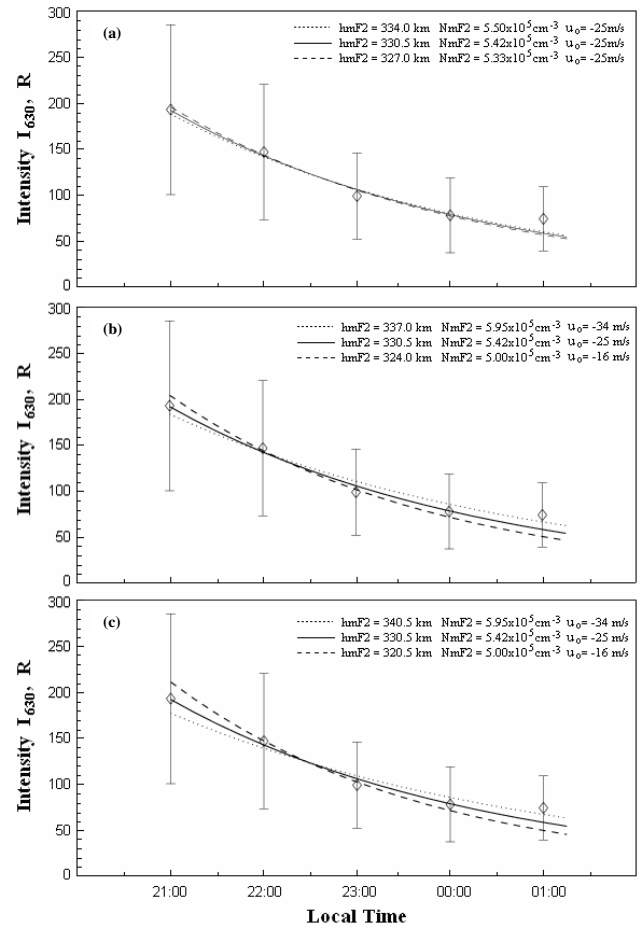

Fig. 4. Night variations of the red line intensity $I_{630}(t)$ observed in April (diamonds) and their theoretical values for the following cases: $u_0=-25$ m/s, decrease in densities of [N_2], [O_2] and [O] by 5% and temperature T_n by 1% (full lines), absence of decrease in the densities of neutrals and temperature (dotted lines), $u_0=-25$ m/s (panel **a**), $u_0=-14$ m/s (panels **b** and **c**), and decrease in the densities of neutrals by 10% and temperature by 2% (dashed lines), $u_0=-25$ m/s (panel b) and $u_0=-34$ m/s (panels **b** and **c**). Vertical lines are one sigma error bars.

temperature T_n for given month and their values [N_2]+δ[N_2], [O_2]+δ[O_2], [O]+δ[O] and T_n+δT_n at different seasons and solar phases. δ[N_2], δ[O_2], δ[O] and δT_n denote changes in the neutral densities and temperature for different seasons and solar phases at some initial height. We use these equations to estimate maximum value in |δI_{630}| for the theoretical red line intensities I_{630} (Eq. 6) plotted in Fig. 4. In this case the value of |δI_{630}|$/I_{630}$ at pre-midnight LT 21:00–22:00 decreases by about 12% for solar maximum phase and increases by up to 30% for the solar minimum phase. It means that the positive trend at LT 21:00–22:00 can possibly get a comparatively smaller value for solar maximum and greater value for solar minimum. The value of |δI_{630}|$/I_{630}$ increases by about 5% at midnight LT 00:00–01:00 for solar

minimum phase and decreases by about the same percentage for maximum phase. In this case the theoretical value of negative trend in the red line intensity at LT 00:00–01:00 should be smaller for solar maximum phase and greater for minimum phase. The value of $|\delta I_{630}|/I_{630}$ is more than twice that of the case where there is no secular decrease (Fig. 4c) in the upper atmosphere neutral gas density. For the seasonal variation $|\delta I_{630}|/I_{630}$ is comparatively smaller for the same meridional wind velocities as in Fig. 4. Note, that more detailed consideration of the daily, seasonal and solar phase depending variations in the red line intensity, which we can easily include in our theoretical formalism, needs the data of thermosphere wind or ion drift velocity over Abastumani.

Figure 4 shows a presence of a positive trend in the red line intensity at pre-midnight (LT 21:00–22:00) and its negative value at midnight/after midnight (LT>23 h), which is caused by a decrease in the neutral gas densities, cooling of the upper atmosphere (Fig. 4a) and a decrease in the southward wind (Fig. 4b and c). The secular decrease in the neutral gas density in the upper atmosphere can give us a comparatively smaller value of the pre-midnight positive and midnight/after midnight negative trend in the red line intensity. In the demonstrated case better agreement between the observed and theoretical estimation of the mean nightly behavior of the red line intensity occurred in the case of the secular decrease in the neutral gas densities and the decrease in the southward wind (Fig. 4b). In next section the latter we will consider as a possible consequence of an increase in the mean daily northward wind.

4 Discussion

The above consideration shows that the positive trend in the oxygen red 630.0 nm line intensity at pre-midnight and its negative value at midnight/after midnight, observed at Abastumani could be caused by negative trend in the peak height hmF2 of the ionosphere F2 layer, which was also observed from the Tbilisi ionosphere station. According to the trend in the hmF2, the nighttime lowering of the ionosphere F2 layer for the time period under consideration is about 15–19 km, which is greater than predicted by Rishbeth (1990), Rishbeth and Roble (1992) assuming global cooling in the upper atmosphere. To explain this observed phenomenon the increase in the northward meridional wind or decrease in the southward is assumed. The daytime meridional wind of the ionosphere F2 region is mainly northward and during nighttime it is southward (Hedin et al., 1991; Buonsanto and Witasse, 1999; Igi et al., 1999). Its daily variations depend on the season, solar phase and are different for different regions (Igi et al., 1999). The negative trend in the hmF2 at the Tbilisi ionosphere station is observed during day and nighttime. In this case the daytime or nighttime lowering in the hmF2 should be a result of the increase in the northward wind velocity. This increase should also cause a decrease in

the nighttime southward wind and the lowering in the hmF2, which was observed during the whole night (Table 1). So, the increase in the northward wind or/and decrease in the southward one shows an increase in the mean annual daily value of the northward wind. The mid-latitude average MLT northward wind velocity increase for some Northern Hemisphere regions is known (Portnyagin et al., 2006).

The nighttime lowering observed in the hmF2 by about 15–19 km should give us higher values in the red line VER $\varepsilon_{630}(h)$ (Eq. 5) and integral intensity $I_{630}(t)$ (Eq. 6) at pre-midnight and its lower value at midnight in the case when there are no changes in the neutral and electron densities for the regions of the luminous layer. Theoretical estimation for night variations of the red line intensity $I_{630}(t)$ (see Fig. 4) is in a comparatively good agreement with the observed positive trend value at pre-midnight LT 21:00–22:00 (Table 1) and its negative value at midnight LT 00:00–01:00 in the case of decrease in the neutral gas density by 10% from 1957 up to 1993, which was chosen according to the secular trend obtained by Emmert et al. (2004). Here the differences in the trends in the red line intensity are caused by the lowering in hmF2 by about 20 km. This lowering in the hmF2 includes the smaller part due to the secular decrease in the neutral gas densities [N_2], [O_2] and [O] by 10%, the upper atmosphere temperature T_n decrease by 2% and lowering due to the decrease in the mean nightly southward wind velocity from 37 m/s to 14 m/s. It was also necessary to assume the presence of a decrease (negative trend) in the NmF2 to satisfy the observational results. In Fig. 4 the decrease in the NmF2 is considered about 10% for LT 20:00–21:00. In our case the negative trend in the NmF2 at Tbilisi ionosphere station was observed for the whole night (Table 1) but it is insignificant.

In present consideration the long-term increase in the average northward thermosphere wind is assumed for explanation of the observed lowering in hmF2. Important changes in the thermosphere wind occurred on magnetically disturbed days as well. The variations in the mid-latitude red line nightglow intensity on magnetically disturbed days is possible to be a result of the increase in the upper atmosphere temperature, the value of the ratio [O]/[N_2] and the increase in the southward wind (Fishkova, 1983; Didebulidze et al., 2002). An increase in the southward wind velocity on magnetically disturbed days affects the upward drift of the ionosphere F2 region plasma and increase in the hmF2 (Mikhailov, 2006). This phenomenon should give us the behavior in the red line nightglow intensity opposite to that of during the increase in the mean northward wind. Even though magnetically disturbed days are rare in comparison with quiet ones the mean annual hmF2 and the red line intensity should be modulated by variations. The regional differences in the geomagnetic field geometry and variations of the thermosphere wind is possible to be reflected in variations of the mid-latitude ionosphere F2 layer parameters (Danilov and Mikhailov, 1999; Mikhailov, 2006, and references therein) and the red line intensity. Simultaneous measurements of these parameters for

a given region increase possibility to quantify the influence of natural and anthropogenic factors in the variations of the upper atmosphere temperature, neutral and charge particle densities and dynamics as well.

Consideration of an increase in the value of the average northward wind (or a decrease in southward one, which is the consequence of the former), gives an increase in the lowering hmF2 up to its observational value at Tbilisi ionosphere station, which was not possible assuming only global cooling in the upper atmosphere. The increase in the northward wind is also possible to be a result of changes in the upper atmosphere dynamics due to global cooling (Rishbeth, 1990). The positive trend at pre-midnight and its negative value at midnight/after midnight in the red 630.0 nm line intensity obtained at Abastumani can be explained by the observed lowering in the hmF2. Thus, the lowering in hmF2 and different nighttime trend values in the red line intensity for the two neighbouring places and their theoretical explanation shows that this phenomenon is possibly caused by cooling in the upper atmosphere, which is considered mostly as a result of an increase in the greenhouse gas densities in the lower atmosphere.

5 Conclusion

Long-term observations of total nightglow intensity of the atomic oxygen red 630.0 nm line at Abastumani in 1957–1993 and measurements of the ionospheric F2 layer parameters from the Tbilisi ionosphere station in 1963–1986 have been analyzed. A change in the long-term trend of the mean annual red line intensity from the pre-midnight positive value ($+0.770 \pm 1.045$ R/year) to the negative value (-1.080 ± 0.670 R/year) at midnight/after midnight has been found. This decrease is accompanied by a lowering of the electron density peak height hmF2 of the ionosphere F2 layer (-0.455 ± 0.343 km/year). The difference in the red line nightglow intensity trends at different times has been considered as a possible result of the lowering observed in the hmF2.

A theoretical simulation using a simple Chapman-type layer (damping in time) for the ionosphere F2 layer electron density has been done. The MSISE90 model has been used for the ionosphere F2 regions neutral particle height distribution. This estimation shows that for satisfaction of the lowering observed in the hmF2, in addition to the decrease in the neutral density and temperature of the upper atmosphere, it is necessary to consider an increase in the northward mean meridional wind velocity (or its possible consequence – a decrease in the southward). The reduction in the neutral density up to 10% corresponding to the secular negative trend obtained by Emmert et al. (2004) has been used. In this case the lowering in hmF2 up to 20 km gives a positive trend in the average annual red line intensity at pre-midnight and its negative value at midnight/after midnight, close to their observational value.

References

Akmaev, R. A.: Thermospheric resistance to "greenhouse cooling": Effect of the collisional excitation rate by atomic oxygen on the thermal response to CO2 forcing, J. Geophys. Res., 108, 1292, doi:10.1029/2003JA009896, 2003.

Akmaev, R. A. and Fomichev, V. I.: Cooling of the mesosphere and lower thermosphere due to the doubling of CO2, Ann. Geophys., 16, 1501–1512, 1998,
http://www.ann-geophys.net/16/1501/1998/.

Bencze, P.: On the long-term change of ionospheric parameters, J. Atmos. Solar-Terr. Phys., 67, 1298–1306, 2005.

Bremer, J.: Trends in the ionospheric E and F regions over Europe, Ann. Geophys., 16, 986–996, 1998,
http://www.ann-geophys.net/16/986/1998/.

Bremer, J. and Berger, U.: Mesospheric temperature trends derived from ground-based LF phase-height observations at midlatitudes: comparison with model simulations, J. Atmos. Solar-Terr. Phys., 64, 805–816, 2002.

Buonsanto, M. J. and Witasse, O. G.: An updated climatology of thermospheric neutral winds and F region ion drifts above Millstone Hill, J. Geophys. Res., 104(A11), 24 675–24 687, 1999.

Danilov, A. D. and Mikhailov, A. V.: Spatial and seasonal variations of the foF2 long-term trends, Ann. Geophys., 17, 1239–1243, 1999,
http://www.ann-geophys.net/17/1239/1999/.

Didebulidze, G. G. and Pataraya, A. D.: Ionosphere F2-region under the influence of the evolutional atmospheric gravity waves in horizontal shear flow, J. Atmos. Solar-Terr. Phys., 61, 479–489, 1999.

Didebulidze, G. G., Chilingarashvili, S. P., Toroshelidze, T. I., Murusidze, I. G., Kvavadze, N. D., and Sharadze, Z. S.: On the possibility of in situ shear excitation of vortical perturbations and their coupling with short-period gravity waves by airglow and ionosphere observations, J. Atmos. Solar-Terr. Phys., 64, 1105–1116, 2002.

Emmert, J. T., Picone, J. M., Lean, J. L., and Knowles, S. H.: Global change in the thermosphere: compelling evidence of a secular decrease in density, J. Geophys. Res., 109, A02301, doi:10.1029/2003JA010176, 2004.

Fishkova, L. M.: The night airglow of the Earth midlatitude upper atmosphere, Metsniereba Press, Tbilisi, 1983 (in Russian).

Givishvili, G. V., Leshchenko, L. N., Lysenko, E. V., Perov, S. P., Semenov, A. I., Sergeenko, N. P., Fishkova, L. M., and Shefov, N. N.: Long-term trends of some characteristics of the Earth's atmosphere. Experimental results, Izvestia AN, Fizika Atmosfery i Okeana, 32(3), 329–39, 1996 (in Russian).

Gudadze, N. B., Didebulidze, G. G., Javakhishvili, G. Sh., Shepherd, M. G., and Vardosanidze, M. V.: Long-term variations of the oxygen red 630 nm line nightglow intensity, Can. J. Phys., 85, 189–198, 2007.

Hedin, A. E.: Extension of the MSIS Thermospheric Model into the Middle and Lower Atmosphere, J. Geophys. Res., 96, 1159–1172, 1991.

Hedin, A. E., Spencer, N. W., Biondi, M. A., Burnside, R. G., Hernandez, G. and Johnson, R. M.: Revised global model of thermosphere winds using satellite and ground-based observations, J. Geophys. Res., 96, 7657–7688, 1991.

Igi, S., Oliver, W. L., and Ogawa, T.: Solar cycle variations of the thermospheric meridional wind over Japan derived from measurements of hmF2, J. Geophys. Res., 104, 22 427–22 431, 1999.

Jarvis, M. J., Jenkins, B., and Rodgers, G. A.: Southern Hemisphere observations of a long-term decrease in F region altitude and thermospheric wind providing possible evidence for global thermospheric cooling, J. Geophys. Res., 103, 20 774–20 787, 1998.

Keating, G. M., Tolson, R. H., and Bradford, M. S.: Evidence of long term global decline in the Earth's thermospheric density apparently related to anthropogenic effects, Geophys. Res. Lett., 27, 1523–1526, 2000.

Lástovička, J., Mikhailov, A. V., Ulich, T., Bremer, J., Elias, A. G., Ortiz de Adler, N., Jara, V., Abarca del Rio, R., Foppiano, A. J., Ovalle, E., and Danilov, A. D.: Long-term trends in foF2: a comparison of various methods, J. Atmos. Solar-Terr. Phys., 68, 1854–1870, 2006.

Marcos, F. A., Wise, J. O., Kendra, M. J., Grossbard, N. J., and Bowman, B. R.: Detection of long-term decrease in thermospheric neutral density, Geophys. Res. Lett., 32, L04103, doi:10.1029/2004GL021269, 2005.

Marin, D., Mikhailov, A. V., de la Morena, B. A., and Herraiz, M.: Long-term hmF2 trends in the Eurasian longitudinal sector on the ground-based ionosonde observations, 2001, Ann. Geophys., 19, 761–772, 2001,
http://www.ann-geophys.net/19/761/2001/.

Marsh, D. N. and Svensmark, H.: Low cloud properties influenced by cosmic rays, Phys. Rev. Lett, 85(23), 5004–5007, 2000.

Megrelishvili, T. G.: Regularities of the variations of the scattered light and emission of the Earth twilight atmosphere, Metsniereba Press, Tbilisi, 1981 (in Russian).

Mikhailov, A. V.: Ionospheric long-term trends: can the geomagnetic and the greenhouse hypotheses be reconciled?, Ann. Geophys., 24, 2533–2541, 2006,
http://www.ann-geophys.net/24/2533/2006/.

Nicolls, M. J., Kelley, M. C., Vlasov, M. N., Sahai, Y., Chau, J. L., Hysell, D. L., Fagundes, P. R., Becker-Guedes, F., and Lima, W. L. C.: Observations and modeling of post-midnight uplifts near the magnetic equator, Ann. Geophys., 24, 1317–1331, 2006,
http://www.ann-geophys.net/24/1317/2006/.

Portnyagin, Yu. I., Merzlyakov, E. G., Solovjova, T. V., Jacobi, Ch., Kürschner, D., Manson, A., and Meek, C.: Long-term trends and year-to-year variability of mid-latitude mesosphere/lower thermosphere winds, J. Atmos. Solar-Terr. Phys., 68, 1890–1901, 2006.

Rishbeth, H.: A greenhouse effect in the ionosphere?, Planet. Space Sci., 38, 945–948, 1990.

Rishbeth, H. and Roble, R. G.: Cooling of the upper atmosphere by enhanced greenhouse gases – Modelling of thermospheric and ionospheric effects, Planet. Space Sci., 40, 1011–1026, 1992.

Roble, R. G. and Dickinson R. E.: How will changes in carbon dioxide and methane modify the mean structure of the mesosphere and thermosphere?, Geophys. Res. Lett., 16, 1441–1444, 1989.

Semeter, J., Mendillo, M., Baumgardner, J., and Holt, J.: A study of oxygen 6300 A airglow production through chemical modification of the nighttime ionosphere, J. Geophys. Res., 101, 19 683–19 699, 1996.

Shimazaki, T.: World-wide variations in the height of the maximum electron density of the ionosphere F2 layer, J. Radio Res. Lab. Jpn., 2(7), 85–97, 1955.

Sobral, J. H. A., Takahashi, H., Abdu, M. A., Muralikrishna, P., Sahai, Y., Zamlutti, C. J., de Paula, E. R.,and Batista, P. P.: Determination of the quenching rate of the O(^{1}D) by O(^{3}P) from rocket-born optical (630 nm) and electron density data, J. Geophys. Res., 98(A5), 7791–7798, 1993.

St.-Maurice, J. P. and Torr, D. G.: Nonthermal rate coefficients in the ionosphere: The reactions of O$^+$ with N$_2$, O$_2$, and NO, J. Geophys. Res., 83, 969–977, 1978.

Tobiska, W. K., Woods, T., Eparvier, F., Viereck, R., Floyd, L., Bouwer, D., Rottman, G., and White, O. R.: The SOLAR2000 empirical solar irradiance model and forecast tool, J. Atmos. Solar-Terr. Phys., 62, 1233–1250, 2000.

Ulich, T. and Turunen, E.: Evidence of long-term cooling of the upper atmosphere in ionosonde data, Geophys. Res. Lett., 24, 1103–1106, 1997.

Xu, Z.-W., Wu, J., Igarashi, K., Kato, H., and Wu, Z.-S.: Long-term ionospheric trends based on ground-based ionosonde observations at Kokubunji, Japan, J. Geophys. Res., 109, A09307, doi:10.1029/2004JA010572, 2004.

Yue, X., Wan, W., Liu, L., Ning, B., and Zhao, B.: Applying artificial neural network to derive long-term foF2 trends in the Asia/Pacific sector from ionosonde observations, J. Geophys. Res., 111, A10303, doi:10.1029/2005JA011577, 2006.